ANALYSIS OF COUPLE STRESS FLUID SQUEEZE FILMS IN CONICAL AND SPHERICAL BEARINGS

M.A.Bedewi
Mechanical Engineering Department, Faculty of Engineering,
El-Minia University, El-Minia, Egypt.

ABSTRACT

A theoretical analysis of non newtonian flow effects in squeeze film configuration is presented with particular reference to conical and spherical bearings. The material model taken is that of the Stokes couple stress fluid. The effects of the material constants of the fluid on the bearing characteristics, namely the load - carrying capacity and film thickness-time relationship, are discussed. It is found that bearings with couple stress fluid as lubricant have greater load - supporting capacities and considerably longer squeeze film time than in the case of newtonian fluid.

1. INTRODUCTION

Non-Newtonian behaviour is observed in various lubrication processes as a consequence of severe operational requirements, use of additives, use of lubricants with long chain molecules or even use of a lubricant contaminated with dust or metal particles. This lubricant containing long chain molecules or suspended particles has to be represented by proper constitutive equations in any theoretical model. Various theories have been proposed to describe the peculiar behaviour of fluids which have a microstructure such as those containing additives, suspensions or granular matter. These theories and their applications have been reviewed by Ariman et al [1,2].

In all microcontinum theories the simplest generalization of the classical fluid mechanics theory to allow for polar effects such as the presence of couple stresses, body couples and a non-symmetric stress tensor is that proposed by Stokes [3]. The basic equations of motion of fluids with couple stress are,

$$\frac{\partial \rho}{\partial t} + \nabla . (\rho V) = 0 \tag{1}$$

$$\rho(\frac{\partial V}{\partial t} + V . \nabla V) = - \nabla P + \rho F + \frac{1}{2}\nabla \times (\rho T) + +(\zeta + \mu + \xi \nabla^2)\nabla(\nabla . V) + (\mu - \xi \nabla^2)\nabla^2 V \tag{2}$$

Where V,F and T are the velocity vector, the body force vector per unit mass and the body couple vector per unit mass, respectively, ρ is the density, P is the pressure, ζ and μ are the classical viscosity coefficients and η is a material constant peculiar to a fluid with couple stress.

This couple stress theory of fluid has found wide application in various lubrication problems [4-9]. It was established theoretically that the presence of additives in the lubricant has significant effect on bearing characteristics, i.e, increases the load capacity and ensures the decrease in coefficient of friction.

The present paper is an extension of the classical squeeze film problems in conical and spherical bearings [10] to the case of fluid lubricants with couple stress.

2. ANALYSIS

When the lubricant is an incompressible couple stress fluid, the inertia forces are negligible and body forces and couples are absent, the governing fluid flow equation (1) and (2) simplify to

$$\nabla . V = 0 \tag{3}$$

$$0 = - \nabla P + \mu \nabla^2 V - \eta \nabla^4 V \tag{4}$$

2.1 Conical Bearing

Imposing the usual assumptions of lubrication theory, the governing equations (3) and (4), in polar co-ordinates, are,

$$\frac{1}{r}\frac{\partial(ru)}{\partial r} + \frac{\partial w}{\partial z} = 0 \qquad (5)$$

$$r - \text{dir } 0 = -\frac{\partial P}{\partial r} + \mu\frac{\partial^2 u}{\partial z^2} - \eta\frac{\partial u^4}{\partial z^4} \qquad (6)$$

The boundary conditions are,

$$u = \frac{\partial^2 u}{\partial z^2} = 0 \quad \text{at } z = 0, H$$
$$w = 0 \qquad \text{at } z = 0 \qquad (7)$$
$$w = \dot{H} = \frac{dH}{dt} = -VE \quad \text{at } z = H$$

Where,

$$E = \sin(\alpha),$$

$$R = Er, \; H = EH_o$$

Solving equation (6) subject to the boundary conditions (7) gives the following velocity distribution,

$$u = \frac{E}{2\mu}\frac{dP}{dR}\left\{z^2 - Hz + 2e^2\left(1 - \frac{\cosh(\frac{2z-H}{2e})}{\cosh(\frac{H}{2e})}\right)\right\} \qquad (8)$$

where,

$$e^2 = \frac{\eta}{\mu}$$

Integration of equation (5) across the fluid film and using equation (8) with the boundary conditions (7) gives the modified Reynolds' equation,

$$\frac{d}{dR}\left\{H^3 R\left(1 - \frac{12e^2}{H^2} + \frac{24e^3}{H^3}\tanh\frac{H}{2e}\right)\frac{dP}{dR}\right\} = -12\frac{\mu VR}{E} \qquad (9)$$

Introducing the dimensionless quantities,

$$\bar{R} = \frac{R}{R_3} \;, \quad \bar{R}_1 = \frac{R_1}{R_3}$$

$$\bar{H} = \frac{H}{R_3} \;, \quad \bar{H}_0 = \frac{H_0}{R_3} \;, \quad \bar{H} = E\bar{H}_0$$

$$\tau = \frac{R_3}{e} \;, \quad k = \frac{1}{\tau^2} \;, \quad \tau H = \frac{H}{e} = \frac{EH_0}{e}$$

$$\bar{P} = \frac{PH_0^3}{\mu R_3^2 V} \;, \quad \bar{F} = \frac{FH_0^3}{\mu R_3^4 V} \;, \quad T = \frac{Ft}{\mu R_3^2}$$

Equation (9) takes the form,

$$\frac{d}{d\bar{R}}\left\{\bar{R}\varphi(\tau, \bar{H})\frac{d\bar{P}}{d\bar{R}}\right\} = -12\frac{\bar{R}}{E^4} \qquad (10)$$

where,

$$\varphi(\tau, \bar{H}) = 1 - \frac{12}{(\tau\bar{H})^2} + \frac{24}{(\tau\bar{H})^3}\tanh\left(\frac{\tau\bar{H}}{2}\right)$$

Integration twice with respect to $(\bar{R})$ yields

$$\bar{P} = -3\frac{\bar{R}^2}{E^4\varphi(\tau,\bar{H})} + \frac{C_1}{\varphi(\tau,\bar{H})}\ln\bar{R} + C_2 \qquad (11)$$

where C_1 and C_2 are integration constants.
Two cases arise;

A full cone and full conical seat, Figure (1-a), and truncated cone and truncated conical seat open at each end, Figure (1-b).

2.1.1. Full cone and Full Conical Seat

In the case of full cone and full conical seat, Figure (1-a), the appropriate boundary conditions of the pressure are,

$$\bar{P} \text{ is finite } \left(\frac{d\bar{P}}{d\bar{R}} = 0\right) \text{ when } \bar{R} = 0 \qquad (12)$$
$$\bar{P} = 0 \qquad \text{when } \bar{R} = 1$$

By using equation (11) with the boundary conditions (12), the pressure distribution is,

$$\bar{P} = \frac{3}{E^4 \varphi(\tau\ ,\ \bar{H})} \{ 1 - \bar{R}^2 \} \tag{13}$$

The load capacity is given by,

$$F = \int_0^{R_3} 2\pi RPdR \tag{14}$$

or in dimensionless form becomes,

$$\bar{F} = \frac{FH_0^3}{\mu V R_3^4} = 2\pi \int_0^1 \bar{P}\ \bar{R}d\bar{R}$$

which on using equation (13) gives,

$$\bar{F} = \frac{3\pi}{2E^4 \varphi(\tau\ ,\ \bar{H})} \tag{15}$$

To obtain the expression for the time of approach let,

$$F = \frac{\mu V R_3^4}{H_0^3} \bar{F} \tag{16}$$

since

$$V = -\frac{dH_0}{dt}$$

then substituting this into equation (16), the nondimensional time of approach is,

$$\Delta T = \frac{Ft}{\mu R_3^2} = \frac{3\pi}{2E^4} \int_{\bar{H}_0}^{\bar{H}_{oi}} \frac{d\bar{H}_o}{\bar{H}_0^3\ \varphi(\tau\ ,\ \bar{H})} \tag{17}$$

For small values of η (or for large τ), equation (10) shows that

$$\varphi(\tau\ ,\ \bar{H}) = 1$$

consequently, equations (13) , (15) and (17) correspond to the classical case of squeeze film configuration with Newtonian fluid [10]. That is,

$$\bar{P} = \frac{3}{E^4} \{ 1 - \bar{R}^2 \} \tag{18}$$

$$\bar{F} = \frac{3\pi}{2E^4} \tag{19}$$

and

$$\Delta T = \frac{3\pi}{4E^4} \{ \frac{1}{\bar{H}_0^2} - \frac{1}{\bar{H}_{oi}^2} \} \tag{20}$$

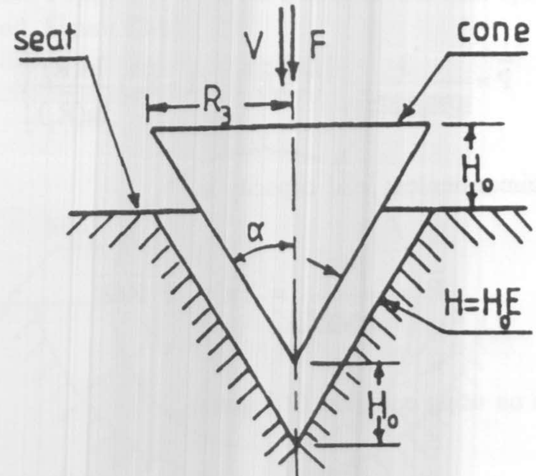

Figure 1-a. Full conical seat.

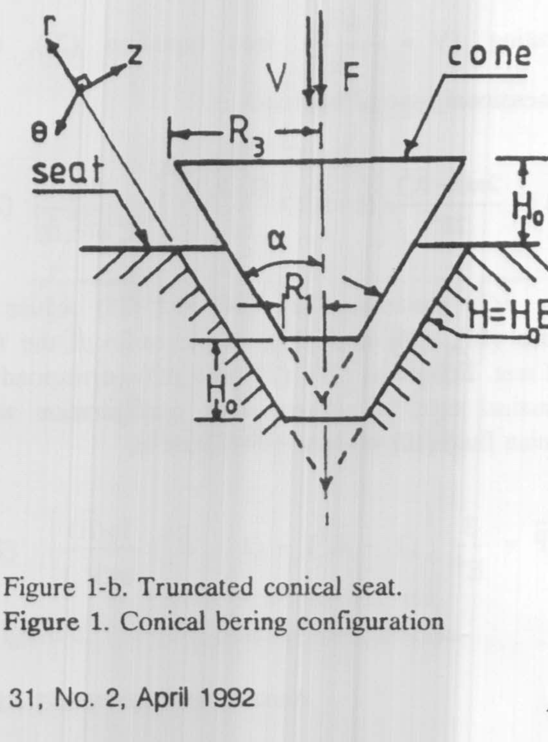

Figure 1-b. Truncated conical seat.
Figure 1. Conical bering configuration

2.1.2. Truncated Cone and Truncated Conical Seat Open at Each End

For the case of truncated cone and truncated conical seat open at each end, Figure (1-b), the appropriate boundary conditions of the pressure are,

$$\bar{P} = 0 \quad \text{when} \quad \bar{R} = \bar{R}_1$$
$$\bar{P} = 0 \quad \text{when} \quad \bar{R} = 1 \qquad (21)$$

By using equation (11) with the boundary conditions (21), the pressure distribution is,

$$\bar{P} = \frac{3}{E^4 \varphi(\tau,\bar{H})}\left\{(1-\bar{R}^2) - (1-\bar{R}_1^2)\frac{\ln(\bar{R})}{\ln(\bar{R}_1)}\right\} \qquad (22)$$

The dimensionless load capacity is,

$$\bar{F} = \frac{FH_0^3}{\mu V R_3^4} = 2\pi \int_{\bar{R}_1}^{1} \bar{P}\,\bar{R}d\bar{R} \qquad (23)$$

which on using equation (22) gives,

$$\bar{F} = \frac{3\pi(1-\bar{R}_1^2)}{2E^4\varphi(\tau,\bar{H})}\left\{(1+\bar{R}_1^2) + \frac{(1-\bar{R}_1^2)}{\ln\bar{R}_1}\right\} \qquad (24)$$

Substituting $(V = -\frac{dH_0}{dt})$ into equation (23), the nondimensional time of approach is,

$$\Delta T = \frac{2\pi(1-\bar{R}_1^2)}{2E^4}\left\{(1+\bar{R}_1^2) + \frac{(1-\bar{R}_1^2)}{\ln\bar{R}_1}\right\}\int_{\bar{H}_0}^{\bar{H}_{0i}} \frac{d\bar{H}_0}{\bar{H}_0^3\,\varphi(\tau,\bar{H})} \qquad (25)$$

If ($\bar{R}_1 = 0$) equations (22), (24) and (25) reduce to equations (13), (15) and (17), respectively, of the full conical seat. Equations (22), (24) and (25) correspond to the classical case of squeeze film configuration with Newtonian fluid [10] when $\tau \rightarrow \infty$. That is,

$$\bar{P} = \frac{3}{E^4}\left\{(1-\bar{R}^2) - (1-\bar{R}_1^2)\frac{\ln(\bar{R})}{\ln(\bar{R}_1)}\right\} \qquad (26)$$

$$,\bar{F} = \frac{3\pi(1-\bar{R}_1^2)}{2E^4}\left\{(1+\bar{R}_1^2) + \frac{(1-\bar{R}_1^2)}{\ln(\bar{R}_1)}\right\} \qquad (27)$$

and
$$\Delta T = \frac{3\pi(1-\bar{R}_1^2)}{4E^4}\left\{(1+\bar{R}_1^2) + \frac{(1-\bar{R}_1^2)}{\ln(\bar{R}_1)}\right\} \times \left\{\frac{1}{\bar{H}_0^2} - \frac{1}{\bar{H}_{0i}^2}\right\} \qquad (28)$$

2.2 Spherical Bearings

Imposing the usual assumptions of lubrication theory, the governing equations (3) and (4), in spherical co-ordinates, are,

$$\frac{1}{\sin(\theta)}\frac{\partial}{\partial\theta}(u\sin(\theta)) + R\frac{\partial w}{\partial z} = 0 \qquad (29)$$

$$8 - \text{dir } 0 = -\frac{1}{R}\frac{\partial P}{\partial\theta} + \mu\frac{\partial^2 u}{\partial z^2} - \eta\frac{\partial^4 u}{\partial z^4} \qquad (30)$$

where,, the radial co-ordinate $r = z + R$ and $R \gg z$, therefore

$$r = R \quad \text{and} \quad \frac{\partial}{\partial r} = \frac{\partial}{\partial z}$$

The boundary conditions are,

$$\left.\begin{aligned} &u = \frac{\partial^2 u}{\partial z^2} = 0 && \text{at } z = 0, H \\ &w = 0 && \text{at } z = H \\ &\text{and } w = \dot{H} = \frac{dH}{dt} = -V\cos(\theta) && \text{at } z = 0 \end{aligned}\right] \qquad (31)$$

Solving equation (30) subject to the boundary conditions (31) gives the velocity distribution as,

$$u = \frac{1}{2\mu R}\frac{dP}{d\theta}\left\{z^2 - Hz + 2e^2\left[1 - \frac{\cosh(\frac{2z-H}{2e})}{\cosh(\frac{H}{2e})}\right]\right\} \qquad (32)$$

where,

$$e^2 = \frac{\eta}{\mu}$$

Integration of equation (29) across the fluid film and using equation (32) with the boundary conditions (31) gives the modified Reynolds' equation,

$$\frac{d}{d\theta}\left\{ \sin(\theta)H^3[1 - \frac{12\epsilon^2}{H^2} + \frac{24\epsilon^3}{H^3}\tanh(\frac{H}{2\epsilon})]\frac{dP}{d\theta}\right\}$$

$$= -6\,\mu R^2\,V\sin(2\theta) \qquad (33)$$

Introducing the dimensionless quantities,

$$\gamma = \frac{e}{C}, \quad \bar{C} = \frac{C}{R}, \quad \bar{H} = \frac{H}{R}$$

$$\tau = \frac{R}{\epsilon}, \quad k = \frac{1}{\tau^2}, \quad \tau\bar{H} = \frac{H}{\epsilon}$$

$$\bar{P} = \frac{PC^3}{\mu R^2 V}, \quad \bar{F} = \frac{FC^3}{\mu R^4 V}, \quad T = \frac{tFC^2}{\mu R^4}$$

equation (33) takes the form

$$\frac{d}{d\theta}\left\{ \sin(\theta)\bar{H}^3\varphi(\tau,\bar{H})\frac{d\bar{P}}{d\theta}\right\} = -6\bar{C}^3\sin(2\theta) \qquad (34)$$

where,

$$\varphi(\tau,\bar{H}) = 1 - \frac{12}{(\tau\bar{H})^2} + \frac{24}{(\tau\bar{H})^3}\tanh(\frac{\tau\bar{H}}{2})$$

From the geometry, given in Figure (2), the film thickness is given by,

$$H = R_o - R - e\cos(\theta) \qquad (35)$$

which can be written as

$$H = C(1 - \gamma\cos(\theta)) \qquad (36)$$

where

$$C = R_o - R, \quad \gamma = \frac{e}{R_o - R}$$

and

$$\bar{H} = \bar{C}(1 - \gamma\cos(\theta)) \qquad (37)$$

Integration of equation (34) twice with respect to θ yields,

$$\frac{d\bar{P}}{d\theta} = -6\frac{\sin(\theta)}{(1-\gamma\cos(\theta))^3\varphi(\tau,\bar{H})} + \frac{A}{(1-\gamma\cos(\theta))^3\sin\theta\,\varphi(\tau,\bar{H})} \qquad (38)$$

and

$$\bar{P} = -6\int\frac{\sin\theta\,d\theta}{(1-\gamma\cos(\theta))^3\varphi(\tau,\bar{H})} + A\int\frac{d\theta}{(1-\gamma\cos(\theta))^3\sin\theta\,\varphi(\tau,\bar{H})} + B \qquad (39)$$

where, (A) and (B) are integration constants. Two cases arise; A sphere in a complete hemispherical seat, Figure (2-a), and a sphere in a partial hemispherical seat open at each end, Figure (2-b).

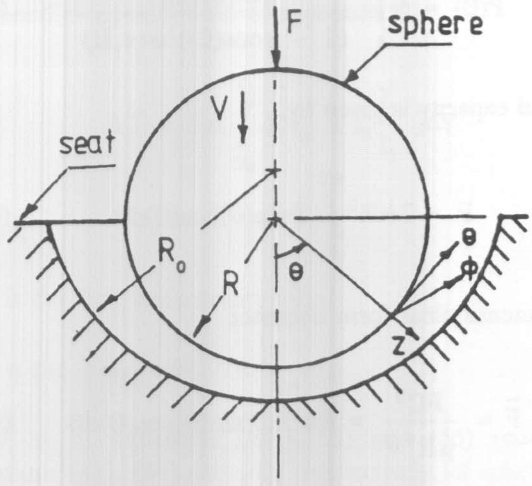

Figure 2-a. Complete hemispherical seat.

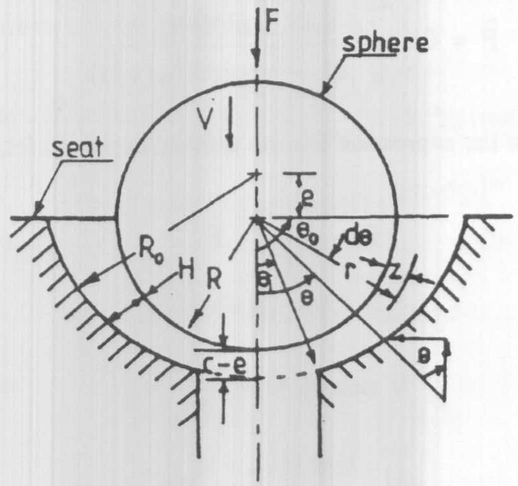

b- Partial hemispherical seat

Figure 2. Spherical bearing configuration.

2.2.1 Sphere in a complete hemispherical seat

In the case of a sphere in a complete hemispherical seat, Figure (2-a), the appropriate boundary conditions of the pressure are,

$$\left.\begin{array}{lll} \frac{d\bar{P}}{d\theta} = 0 & \text{when} & \theta = 0 \\ \bar{P} = 0 & \text{when} & \theta = \pi/2 \end{array}\right] \quad (40)$$

by using equation (38) and (39) with the boundary conditions (40), the pressure distribution is,

$$\bar{P}(\theta) = 6\int_{\theta}^{\pi/2} \frac{\sin(\theta)\, d\theta}{(1 - \gamma\cos(\theta))^3\varphi(\tau,\bar{H})} \quad (41)$$

The load capacity is given by,

$$F = 2\pi R^2 \int_0^{\pi/2} P\sin(\theta)\cos(\theta)d\theta \quad (42)$$

or in dimensionless form becomes

$$\bar{F} = \frac{FC^3}{\mu R^4 V} = 6\pi \int_0^{\pi/2} \bar{P}\sin(\theta)\cos(\theta)d\theta \quad (43)$$

which on using equation (41) gives,

$$\bar{F} = 6\pi \int_0^{\pi/2} \frac{\sin^3(\theta)d\theta}{(1 - \gamma\cos(\theta)^3\varphi(\tau,\bar{H})} \quad (44)$$

To obtain the expression for the time of approach let,

$$F = \frac{\mu R^4 V}{C^3}\bar{F} \quad (45)$$

since,

$$V\cos(\theta) = -\frac{dH}{dt}$$

$$,\frac{dH}{dt} = -C\cos(\theta)\frac{d\gamma}{dt}$$

Thus,

$$V = C\frac{d\gamma}{dt} \quad (46)$$

Substituting equations (46) and (44) into equation (45), the nondimensional time of approach is,

$$\Delta T = \frac{C^3 F}{\mu R^4}\Delta t = 6\pi \int_{\gamma_0}^{\gamma_1}\int_0^{\pi/2} \frac{\sin^3(\theta)d\theta}{(1 - \gamma\cos(\theta))^3\varphi(\tau,\bar{H})} \quad (47)$$

For small values of η (or for large τ), equation (34) shows that,

$$\varphi(\tau,\bar{H}) = 1$$

consequently, equations (41), (44) and (47) correspond to the classical case of squeeze film configuration with Newtonian fluid [10]. That is,

$$\bar{P}(\theta) = \frac{3}{\gamma}\left\{\frac{1}{(1 - \gamma\cos(\theta))^2} - 1\right\} \quad (48)$$

$$,\quad \bar{F} = 6\pi\left\{\frac{1}{\gamma^2(1-\gamma)} + \frac{1}{\gamma^3}\ln(1-\gamma) - \frac{1}{2\gamma}\right\} \quad (49)$$

$$\text{and } \Delta T = -3\pi\left\{\frac{1}{\gamma} + \left(\frac{\gamma^2+1}{\gamma^2}\right)\ln(1-\gamma)\right\}_{\gamma_0}^{\gamma_1} \quad (50)$$

In this case, when the center of the sphere and hemispherical seat coincide ($\gamma = 0$) the values of the expressions in the square brackets in equation (49) and (50) becomes (2/3) and (- 1/2) respectively.

2.2.2. A Sphere in a partial hemispherical seat open at each end.

In the case of a sphere in a partial hemispherical seat open at each end, Figure (2-b), the appropriate boundary conditions of the pressure are,

$$\begin{array}{lll} \bar{P} = 0 & \text{when} & \theta = \theta_i \\ \bar{P} = 0 & \text{when} & \theta = \pi/2 \end{array} \quad (51)$$

By using equation (38) and (39) with the boundary conditions (51), the pressure distribution is,

$$\bar{P}(\theta) = 6\int_{\theta}^{\pi/2} \frac{\sin(\theta)d\theta}{(1-\gamma\cos(\theta))^3\varphi(\tau,\bar{H})} - A\int_{\theta}^{\pi/2} \frac{d\theta}{(1-\gamma\cos(\theta))^3\sin(\theta)\varphi(\tau,\bar{H})} \qquad (52)$$

where,

$$A = 6\,\frac{\displaystyle\int_{\theta_i}^{\pi/2} \frac{\sin(\theta)d\theta}{1-\gamma\cos(\theta))^3\varphi(\tau,\bar{H})}}{\displaystyle\int_{\theta_i}^{\pi/2} \frac{d\theta}{(1-\gamma\cos(\theta))^3\sin(\theta)\varphi(\tau,\bar{H})}}$$

The angle of separation (λ) at which maximum pressure occurs may be obtained from equation (38), where $\frac{d\bar{P}}{d\theta} = 0$ at $\theta = \lambda$, as

$$\sin^2(\gamma) = \frac{\displaystyle\int_{\theta_i}^{\pi/2} \frac{\sin(\theta)d\theta}{(1-\gamma\cos(\theta))^3\theta(\tau,\bar{H})}}{\displaystyle\int_{\theta_i}^{\pi/2} \frac{d\theta}{(1-\gamma\cos(\theta))^3\sin(\theta)\varphi(\tau,\bar{H}}} \qquad (53)$$

The dimensionless load capacity is,

$$\bar{F} = \frac{FC^3}{\mu R^4 V} = 6\pi\int_{\theta_i}^{\pi/2} \bar{P}\sin(\theta)\cos(\theta)d\theta \qquad (54)$$

which on using equation (52) gives,

$$\bar{F} = 6\pi\,[I_4 - I_5\,.\,I_6\,] \qquad (55)$$

where,

$$I_1 = \int_{\theta_i}^{\pi/2} \frac{\sin^3(\theta)d\theta}{(1-\gamma\cos(\theta))^3\varphi(\tau,\bar{H})}$$

$$,\ I_2 = \int_{\theta_i}^{\pi/2} \frac{\sin(\theta)d\theta}{(1-\gamma\cos(\theta))^3\varphi(\tau,\bar{H}}$$

$$,\ I_3 = 6\pi\int_{\theta_i}^{\pi/2} \frac{d\theta}{\sin\theta\,(1-\gamma\cos(\theta))^3\varphi(\tau,\bar{H})}$$

$$,\ I_4 = I_1 - I_2\sin^2(\theta_i)$$

$$,\ I_5 = I_2 - I_3\sin^2(\theta_i)$$

and

$$I_6 = \frac{I_2}{I_3}$$

Substituting equations (46) and (55) into equation (45), the nondimensional time of approach is,

$$\Delta T = 6\pi\int_{\gamma_0}^{\gamma_1} [\,I_4 - I_5\frac{I_2}{I_3}\,]d\gamma \qquad (56)$$

where,

γ_1 is the final eccentricity ratio.

γ_0 is the initial eccentricity ratio.

If (θ_i = 0) equations (52), (55) and (56) reduce to equations (41), (44) and (47), respectively, of sphere in a complete hemispherical seat.

Equations (52), (55) and (56) correspond to the classical case of squeeze film configuration with Newtonian fluid [10] when τ tends to infinity. That is,

$$\bar{P}(\theta) = \frac{6}{2\gamma}\left\{\frac{-1}{(1-\gamma.\cos\theta)^2}\right\}_{\theta}^{\pi/2} - \frac{A}{(1-\gamma^2)^3}\left\{(1+3\gamma^2)\ln|\tan(\frac{b}{2})|\right. \qquad (57)$$

$$\left.\gamma(3+\gamma^2)\ln|\sin(b)| + \gamma^2\cos(b)(3-\frac{\gamma\cos(b)}{2})\right\}_{b_2}^{b_1}$$

$$,\bar{F} = 6\pi[I_4 - I_5\,.\,I_6] \qquad (58)$$

where

$$\varphi(\tau\ ,\ \bar{H}) = 1$$

and

$$I_1 = \frac{1}{2\gamma}\left\{\frac{\sin^2(\theta_i)}{(1-\gamma\cos(\theta_i))^2} + \frac{2\cos(\theta_i)}{\gamma(1-\gamma\cos(\theta_i))} + \frac{2}{\gamma^2}\ln(1-\gamma\cos(\theta_i)) - 1\right\}$$

$$, I_2 = \frac{1}{2\gamma}\left\{\frac{1}{(1-\gamma\cos(\theta_i))^2} - 1\right\}$$

and

$$I_3 = \frac{-1}{(1-\gamma^2)^3}\left\{(1+3\gamma^2)\ln\left|\tan\left(\frac{b}{2}\right)\right| + \gamma^2\cos(b)\left(3 - \frac{\gamma\cos(b)}{2}\right) - \gamma(3+\gamma^2)\ln\left|\sin(\right.\right.$$

where,

$$b_1 = \cos^{-1}\frac{\gamma - \cos(\theta_i)}{1-\gamma\cos(\theta_i)} \quad \text{when} \quad \theta = \theta_i$$

$$, b_2 = \cos^{-1}(\gamma) \quad \text{when} \quad \theta = \pi/2$$

3. RESULTS AND DISCUSSION

3.1 Couple stress parameter

The couple stress fluid is characterized by the two material constants μ and η, the dimensions of μ are those of viscosity whereas the dimensions of η are those of momentum . The ratio (η/μ) has dimensions of length squared. The non-dimensional parameter τ defined by $\tau = R\,(\mu/\eta)^{1/2}$, where R is a typical dimension of the flow geometry, characterizes the couple stress property of the fluid and also distinguishes it from the newtonian fluid. If $(\eta/\mu)^{1/2}$ is a function of molecular dimensions and can be identified with a property which depends on the size of molecule, such as the chain length of the molecule of a polar additive in a non-polar lubricant, it will vary for different liquids. Such a "size dependent effect"does not exist in non-polar fluids. Therefore the parameter τ provides a mechanism which might be helpful in explaining some of the rheological abnormalities that are commonly observed in certain fluids containing additives when the flows are confined to narrow gaps.

When τ is small, which implies that either the characteristic material length $(\eta/\mu)^{1/2}$ is large or the geometric length is small, couple stresses which arise as a consequence of the intrinsic motion of the lubricant or additive molecule are likely to be more significant. Thus the smaller τ is, the more pronounced are the effects due to couple stresses. Moreover, the linear theory of polar fluids should be more accurate than linear viscous fluid theory. For large values of τ either the characteristic material length $(\eta/\mu)^{1/2}$ is small or the geometric length is large, couple stresses are not likely to be significant which in turn implies that the bearing characteristics reduce to their equivalents in Newtonian theory.

3.2 Bearing Characteristics

3.2.1 Conical Bearing

Dimensionless pressure distribution, load carrying capacity and time of approach are shown in graphical form in Figures (3-9) for a wide range of the couple stress parameter τ and two values of semi-vertical cone angle α (E = 0.5, 1.0). These curves are drawn for full and truncated conical seats ($\bar{R}_1$ = 0.0, 0.25). As $\tau \to \infty$, we arrive at the classical Newtonian fluid theory.

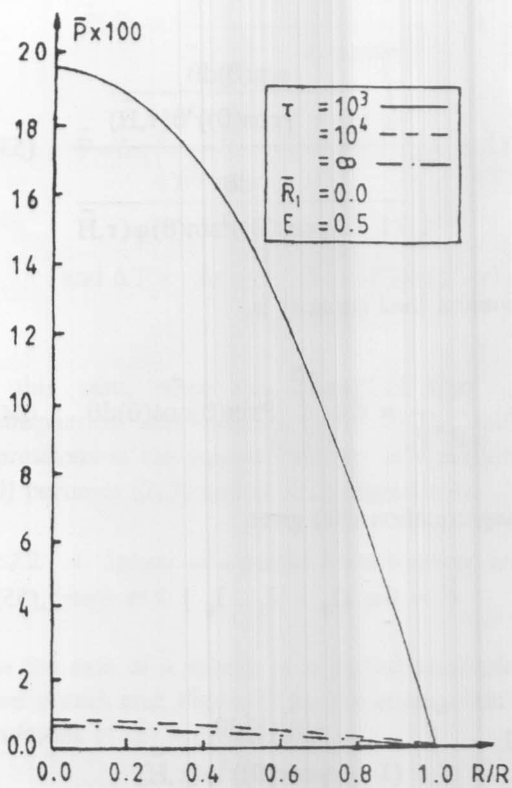

Figure 3. Dimensionless pressure distribution for various values of couple stress parameter (τ), full conical seat.

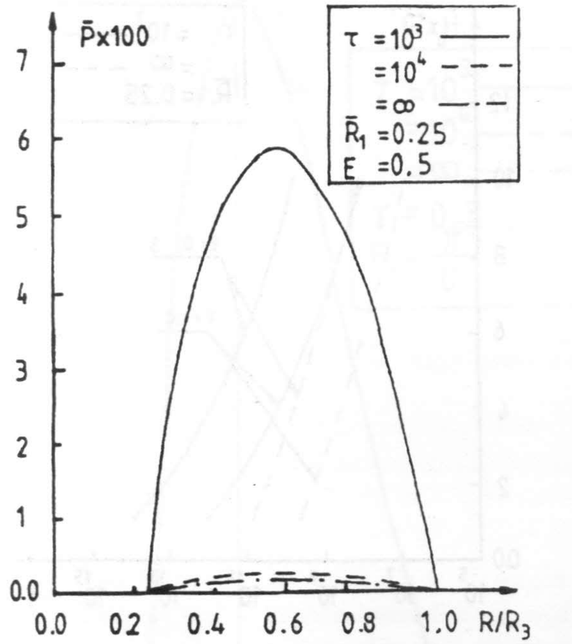

Figure 4. Dimensionless pressure distribution for various values of couple stress parameter (τ), truncated conical seat.

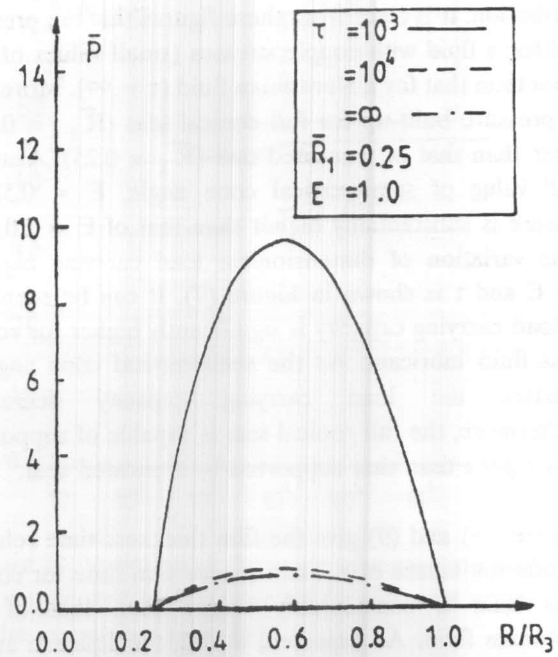

Figure 6. Dimensionless pressure distribution for various values of couple stress parameter (τ), plane annular discs.

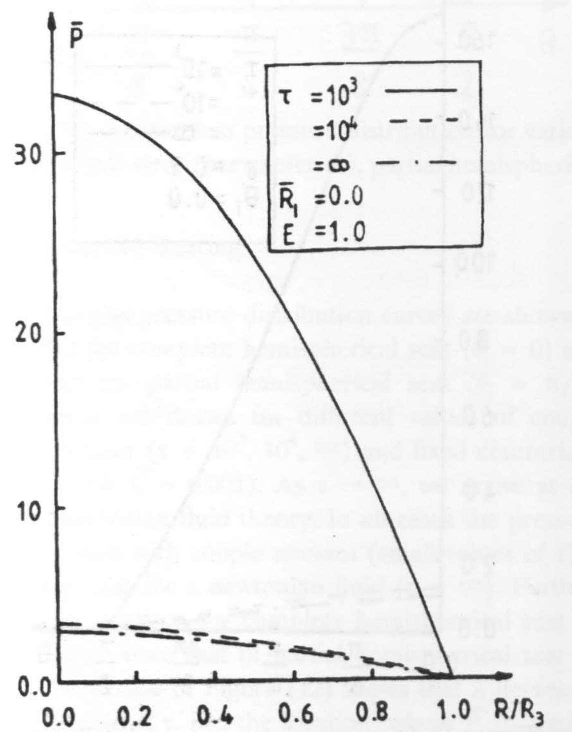

Figure 5. Dimensionless pressure distribution for various values of couple stress parameter (τ), plane dises.

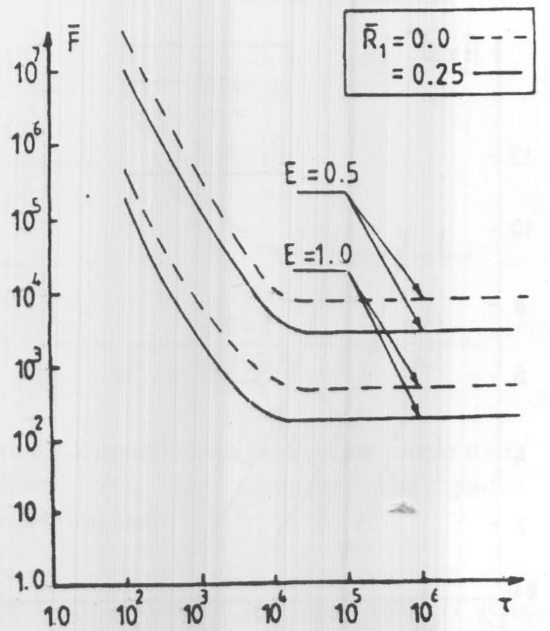

Figure 7. Dimensionless load versus couple stress parameter (τ) for full and truncated conical seat at different values of cone angle.

Figures (3) - (6) show the dimensionless pressure distribution. It is clear from these figures that the pressure level for a fluid with couple stresses (small values of τ) is higher than that for a Newtonian fluid ($\tau = \infty$). Moreover, the pressure built-up for full conical seat ($\bar{R}_1 = 0.0$) is higher than that of truncated one ($\bar{R}_1 = 0.25$). Also, for small value of semi-vertical cone angle, E = 0.5, the pressure is substantially higher than that of E = 1.0.

The variation of dimensionless load carrying capacity with E and τ is shown in Figure (7). It can be seen that the load carrying capacity is significantly higher for couple stress fluid lubricant. As the semi-vertical cone angle α increases the load carrying capacity decreases. Furthermore, the full conical seat is capable of supporting loads higher than that supported by truncated seat.

Figures (8) and (9) give the film thickness-time relation for different values of τ. The squeeze film time for couple stress fluid is considerably longer than that of the Newtonian fluid. As expected, during the squeeze action a cone on a truncated conical seat sinks more quickly through the film than an equivalent one on a full conical seat. Further, a large value of semi-vertical cone angle α results in much less time needed for reducing the film thickness a certain value from a specific position.

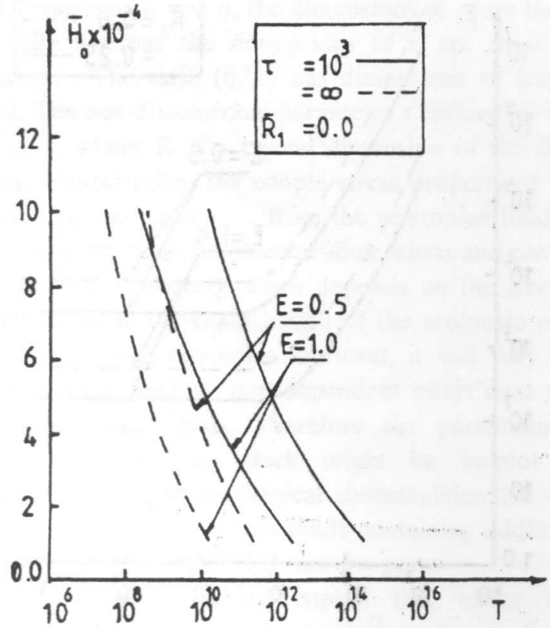

Figure 8. Dimensionless time versus film thickness for various values of couple stress parameter (τ), full conical scat.

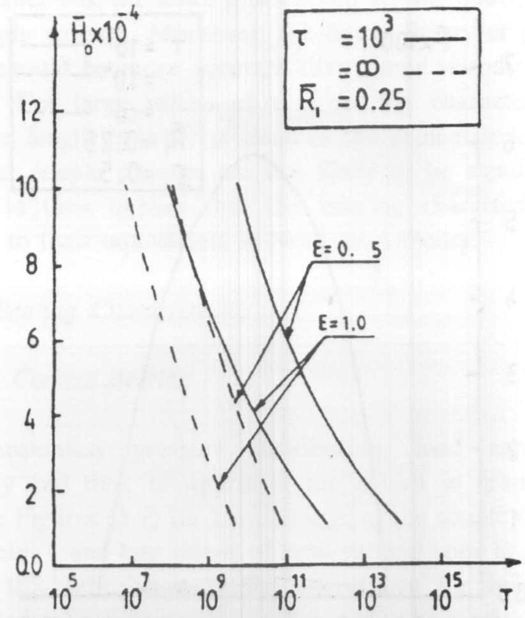

Figure 9. Dimensionless time versus film thickness for various values of couple stress parameter (τ), truncated conical scat.

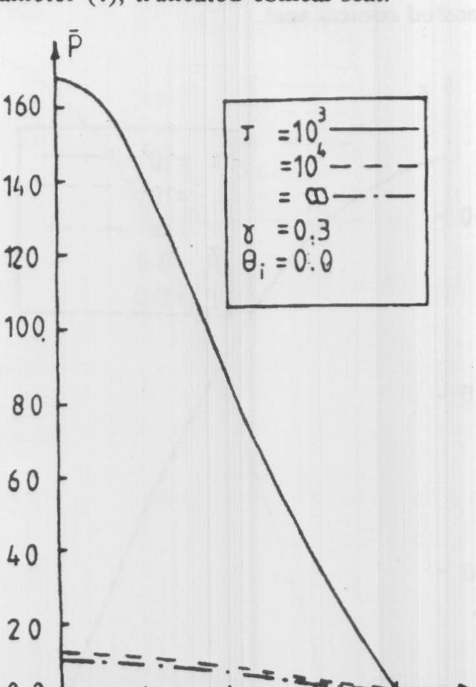

Figure 10. Dimensionless pressure distribution for various values of couple stress parameter (τ), complete hemispherical seat.

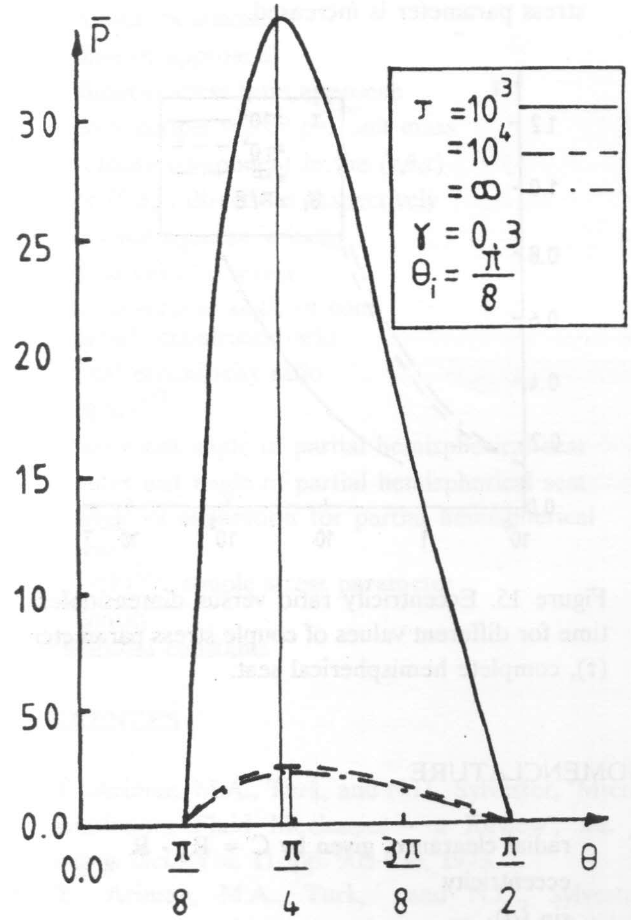

Figure 11. Dimensionless pressure distribution for various values of couple stress parameter (τ), partial hemispherical seat.

3.2.2 Spherical Bearings

Dimensionless pressure distribution curves are shown in Figure (10) for complete hemispherical seat (θ_i = 0) and Figure (11) for partial hemispherical seat ($\theta_i = \pi/8$). These curves are drawn for different values of couple stress parameter ($\tau = 10^3, 10^4, \infty$) and fixed eccentricity ratio (γ = 0.3, $\bar{C}$ = 0.001). As $\tau \rightarrow \infty$, we arrive at the classical Newtonian fluid theory. In all cases the pressure level for a fluid with couple stresses (small values of τ) is higher than that for a newtonian fluid ($\tau = \infty$). Further, the pressure built-up for complete hemispherical seat (θ_i = 0) is higher than that of partial hemispherical seat ($\theta_i = \pi/8$). Inspection of Figure (12) shows that λ decreases with decreasing of τ, i.e., the location where $\bar{P}_{max}$ exsists shifts closer to the inner edge of the partial hemispherical seat. Also inspection of the same Figure shows that at the same value of τ, λ decreases with increasing of γ.

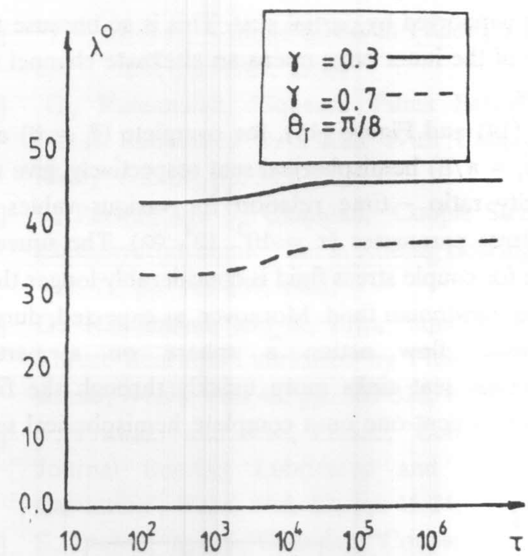

Figure 12. Variation of the angle of separation with the couple stress parameter (τ) for different values of the eccentriaty ratio (γ).

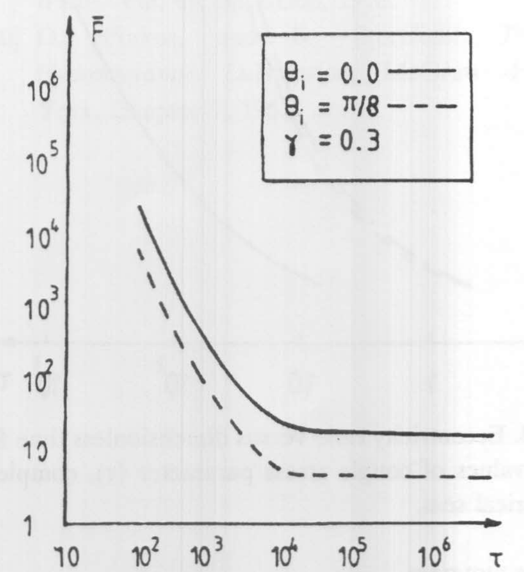

Figure 13. Dimensionless load versus couple stress parameter (τ), for complete and partial hemispherical seat.

Figure (13) shows the dimensionless load capacity versus couple stress parameter τ at fixed value of eccentricity ratio (γ = 0.3), for complete (θ_i = 0) and partial (θ_i = $\pi/8$) hemispherical seats. It is clear from the figure that the couple stress parameter τ has an adverse effect on the load capacity. It is also evident that the complete hemispherical seat is capable of supporting loads higher than that supported by partial seat. This is so because the presence of the inner edge opens an alternate channel for fluid flow.

Figure (14) and Figure (15), for complete ($\theta_i = 0$) and partial ($\theta_i = \pi/8$) hemispherical seat respectively, give the eccentricity ratio - time relation for various values of couple stress parameter ($\tau = 10^3, 10^4, \infty$). The squeeze film time for couple stress fluid is considerably longer than that of the newtonian fluid. Moreover, as expected, during the squeeze flow action a sphere on a partial hemispherical seat sinks more quickly through the film than an equivalent one on a complete hemispherical seat

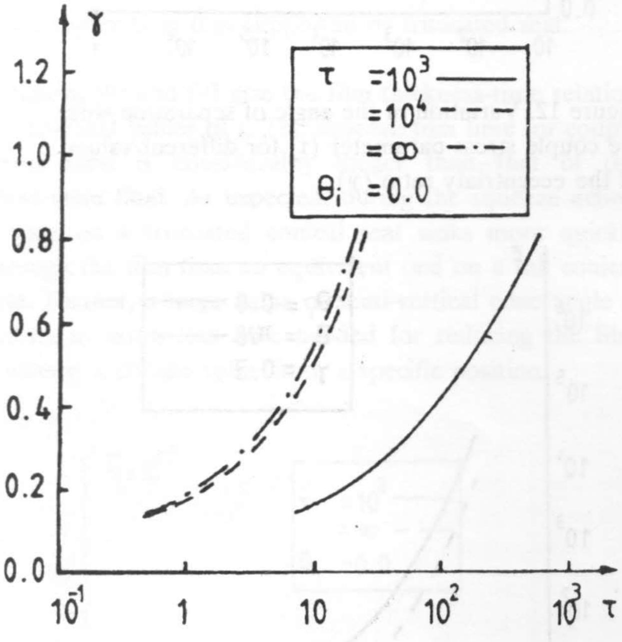

Figure 14. Eccentricity ratio versus dimensionless time for different values of couple stress parameter (τ), complete hemispherical seat.

4. CONCLUSIONS

Analysis of couple stress fluid squeeze films in conical and spherical bearings lead to the following conclusions:

1 - The load capacity of couple stress fluid is significantly higher than that of Newtonian fluid.

2 - The load capacity is decreased as the couple stress parameter is increased.

3 - Squeeze action in fluids with couple stress is slower than in Newtonian fluids.

4 - The time of approach is decreased as the couple stress parameter is increased.

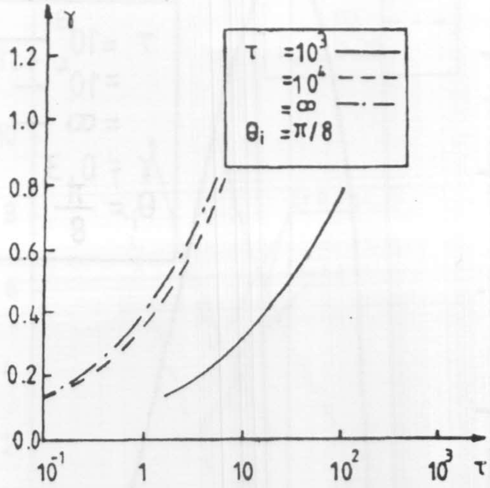

Figure 15. Eccentricity ratio versus dimensionless time for different values of couple stress parameter (τ), complete hemispherical seat.

NOMENCLATURE

C	radial clearance, given by $C = R_o - R$
e	eccentricity
E	sin (α)
F	load capacity
F	force vector per unit mass
$\overline{F}$	dimensionless load capacity
H	oil film thickness
H_o	distance between vertices of the cones
H_{oi}	initial film thickness
$\overline{H}$	dimensionless oil film thickness
k	$\eta/\mu R_3^2$ (conical bearings) $\eta/\mu R^2$ (spherical bearings)
P	pressure
$\overline{P}$	dimensionless pressure
r,θ,z	cylindrical coordinates system
r,θ,ϕ	spherical coordinates system
R	r sin (α), horizontal coordinate in the case of conical bearings
	radius of sphere in the case of spherical bearings
R_0	radius of hemispherical seat
R_1	radius of the base of truncated side of cone
R_3	radius of the base of the cone
$\overline{R}$	dimensionless horizontal coordinate in the case of

conical bearings
t time of approach
T dimensionless time approach
T body couple vector per unit mass
u,v,w velocity component in the (r,θ,z) or (θ,ϕ,r) directions respectively
V normal squeeze velocity
V fluid velocity vector
α semi-vertical angle of cone
γ_0 initial eccentricity ratio
γ_1 final eccentricity ratio
ϵ $(\eta/\mu)^{1/2}$
θ_i inner exit angle of partial hemispherical seat
θ_0 outer exit angle of partial hemispherical seat
λ angle of separation for partial hemispherical seat
τ $1/(k)^{1/2}$, couple stress parameter
ρ density
ζ,μ,η material constants

REFERENCES

[1] T., Ariman, M.A., Turk, and N.D., Sylvester, "Microcontinuum Fluid Mechanics - a Review", *Int. J. engng. Sci.*, Vol. 11, pp. 905-930, 1973.

[2] T., Ariman, M.A., Turk, and N.D., Sylvester, "Applications of Microcontinuum Fluid Mechanics", *Int. J. Engng. Sci.*, Vol. 12, pp. 273-293, 1974.

[3] V.K., Stokes, "Couple Stress in Fluids", *The physics of Fluids* 9, pp. 1709, 1966.

[4] G., Ramanaiah, "Squeeze Films Between Finite Plates Lubricated by Fluids With Couple Stress", *Wear*, Vol. 54, pp. 315-320, 1979.

[5] S., Parwal, and S., Chandan, "Couple Stress in the Elastohydrodynamic Film in Rolling Bearings", *Wear*, Vol. 71, pp. 129-137, 1981.

[6] G., Ramanaiah, and S., Priti, "Squeeze Films and Thrust Bearings Lubricated by Fluids with Couple stress", *Wear*, Vol. 48, pp. 309-316, 1978.

[7] S., Prawal, and K.R., Prasad, "Couple Stresses in Journal Bearing Lubricated and the Effect of Cavitation", *Wear*, Vol. 67, pp. 15-24, 1981.

[8] S., Prawal, and S., Chandan, "Couple Stresses in the Lubrication of Rolling Contact Bearings Considering Cavitation", *Wear*, vol. 67, pp. 85-98, 1981.

[9] G., Ramanaiah, "Optimum Load Capacity of a Slider Bearing Lubricated by a Fluid with Couple Stress", *Wear* Vol. 49, pp. 61-66, 1978.

[10] O., Pinkus, and B., Sternlicht, *Theory of Hydrodynamic Lubrication*, McGraw -Hill, New York, Chapter 7, 1961.